Constitutive WNT/Beta-Catenin Signaling in Murine Sertoli Cells Disrupts Their Differentiation and Ability to Support Spermatogenesis 1

Authors: Tanwar, Pradeep S., Kaneko-Tarui, Tomoko, Zhang, LiHua, Rani, Poonam, Taketo, Makoto M., et al.

Source: Biology of Reproduction, 82(2) : 422-432

Published By: Society for the Study of Reproduction

URL: https://doi.org/10.1095/biolreprod.109.079335

BIOLOGY OF REPRODUCTION **82,** 422–432 (2010)
Published online before print 30 September 2009.
DOI 10.1095/biolreprod.109.079335

Constitutive WNT/Beta-Catenin Signaling in Murine Sertoli Cells Disrupts Their Differentiation and Ability to Support Spermatogenesis[1]

Pradeep S. Tanwar,[3] Tomoko Kaneko-Tarui,[3] LiHua Zhang,[3] Poonam Rani,[3] Makoto M. Taketo,[4] and Jose Teixeira[2,3]

Vincent Center for Reproductive Biology,[3] Department of Obstetrics, Gynecology, and Reproductive Biology, Massachusetts General Hospital and Harvard Medical School, Boston, Massachusetts
Department of Pharmacology,[4] Graduate School of Medicine, Kyoto University, Yoshida-Konoe-cho, Sakyo, Kyoto, Japan

ABSTRACT

Sertoli and germ cell interactions are essential for spermatogenesis and, thus, male fertility. Sertoli cells provide a specialized microenvironment for spermatogonial stem cells to divide, allowing both self-renewal and spermatogenesis. In the present study, we used mice with a conditional activated allele of the beta-catenin gene (*Ctnnb1*$^{tm1Mmt/+}$) in Sertoli cells expressing Cre recombinase driven by the anti-Müllerian hormone (AMH; also known as Müllerian-inhibiting substance) type II receptor promoter (*Amhr2*$^{tm3(cre)Bhr/+}$) to show that constitutively activated beta-catenin leads to their continuous proliferation and compromised differentiation. Compared to controls, Sertoli cells in mature mutant mice continue to express high levels of both AMH and glial cell-derived neurotrophic factor (GDNF), which normally are expressed only in immature Sertoli cells. We also show evidence that LiCl treatment, which activates endogenous nuclear beta-catenin activity, regulates both AMH and GDNF expression at the transcriptional level. The epididymides were devoid of sperm in the *Amhr2*$^{tm3(cre)Bhr/+}$; *Ctnnb1*$^{tm1Mmt/+}$ mice at all ages examined. We show that the mutant mice are infertile because of defective differentiation of germ cells and increased apoptosis, both of which are characteristic of GDNF overexpression in Sertoli cells. Constitutive activation of beta-catenin in *Amhr2*-null mice showed the same histology, suggesting that the phenotype was the result of persistent overexpression of GDNF. These results show that dysregulated wingless-related MMTV integration site/beta-catenin signaling in Sertoli cells inhibits their postnatal differentiation, resulting in increased germ cell apoptosis and infertility.

anti-Müllerian hormone, apoptosis, glial cell-derived neurotrophic factor, gonocyte, Müllerian-inhibiting substance, Sertoli cells, spermatogenesis, testis

INTRODUCTION

Spermatogonial stem cells (SSCs; also known as A_{single} [A_s] spermatogonia in mice) reside at the basal compartment of seminiferous tubules of mammalian testis, where they divide to self-renew or to produce committed progenitor cells known as A_{paired} (A_{pr}) spermatogonia. The A_{pr} spermatogonia continue to divide to form more differentiated spermatogonia that ultimately give rise to mature spermatozoa during spermatogenesis [1]. In normal adult testicular tissue homeostasis, SSCs maintain a balance between self-renewal and differentiation, because an excess of either process will lead to infertility [1]. Excessive self-renewal would lead to a lack of A_{pr}, whereas excessive differentiation would result in exhaustion of SSCs. Thus, these two processes are tightly controlled by intrinsic signals of SSCs and extrinsic signals from the microenvironment, known as the SSC niche. The SSC niche is formed by Sertoli cells, the only somatic cells found inside the seminiferous tubules. During development, these cells play an essential role in testicular morphogenesis. Along with genetic evidence, colocalization of SSCs and Sertoli cells has provided support for the role of Sertoli cells in maintenance of the SSC niche [2–6].

β-Catenin is a key mediator of the wingless-related MMTV integration site (WNT) pathway [7, 8]. WNTs are a family of secreted proteins involved in regulation of a variety of developmental processes [9], including determination of segment polarity during *Drosophila* larval development [10], axis specification in *Xenopus* [11], and differentiation of brain [12], kidney [13], and limb [14] as well as reproductive tracts of male and female mice [15, 16]. WNTs bind to their respective cell surface frizzled/low-density lipoprotein receptor-related protein (LRP) receptors and induce signal transduction through three known pathways: the canonical WNT/β-catenin pathway, the noncanonical polarity pathway, and the WNT/Ca^{2+} pathway. In the canonical pathway, β-catenin normally is found in the cytoplasm of cells, often coupled to adherens junctions [17]. The stability of free β-catenin in the cytoplasm is regulated by destruction complex formed by axin, adenomatosis polyposis complex, casein kinase 1, and glycogen synthase kinase 3-β (GSK3B). This multiprotein complex phosphorylates β-catenin, leading to its ubiquitination and proteolytic destruction. During canonical WNT signaling, axin is recruited to the phosphorylated tail of LRP and/or to frizzle-bound dishevelled, leading to the inhibition of kinase activity of adenomatosis polyposis complex. This causes accumulation of β-catenin in cytoplasm, which translocates to the nucleus to activate WNT-regulated transcription of various targeted genes [7, 9].

WNT signaling in the testis has not been well studied, but it has been shown to play an important role in proliferation and self-renewal of mouse and human spermatogonia [18]. Recently, Boyer et al. [19] reported that expression of a constitutively activated form of β-catenin in postnatal Sertoli

[1]Supported in part by a grant from the NICHD (HD052701).
[2]Correspondence: Jose Teixeira, Vincent Center of Reproductive Biology/Thier 931, Massachusetts General Hospital and Harvard Medical School, 55 Fruit St., Boston, MA 02114.
FAX: 617 726 0561; e-mail: teixeira@helix.mgh.harvard.ed

Received: 8 June 2009.
First decision: 9 July 2009.
Accepted: 16 September 2009.

eISSN: 1529-7268 http://www.biolreprod.org
ISSN: 0006-3363

cells causes male infertility via progressive deterioration of seminiferous tubules, germ cell loss, and testicular atrophy. In the present study, we have investigated the molecular mechanisms involved in constitutive β-catenin signaling in postnatal Sertoli cells using the same mouse model. Our results show that expression of constitutively activated β-catenin maintains Sertoli cells in the postnatal testis in an immature state. In particular, we provide evidence that the immature Sertoli cell phenotype is caused by persistent expression of glial cell-derived neurotrophic factor (GDNF), a member of the transforming growth factor β family of growth and differentiation factors and a master regulator of spermatogenesis [4].

MATERIALS AND METHODS

Mouse Genetics and Husbandry

The mice used in the present study were kept under standard animal housing conditions. The Institutional Animal Care and Use Committee at Massachusetts General Hospital approved all protocols involving animal experimentation. All mice used in the present study were maintained on C57BL/6;129/SvEv mixed genetic background. *Amhr2*$^{tm3(cre)Bhr/+}$ mice [20] were mated with *Ctnnb1*$^{tm1Mmt/tm1Mmt}$, which encodes phosphorylation sites required for its degradation by the adenomatosis polyposis complex [21], to generate *Amhr2*$^{tm3(cre)Bhr/+}$;*Ctnnb1*$^{tm1Mmt/+}$ mice. The genetic crosses used to generate *Amhr2-cre*/+;*YFP*/+ has been described previously [16, 22]. Genotyping was performed on DNA from tail biopsies using standard PCR protocols. The age of embryos was determined by the day on which a vaginal plug was detected (considered to be Embryonic Day 0.5). The Embryonic Day 14, 16, and 18 as well as the 1-day-old and 8-wk-old testes were collected from *Amhr2*$^{tm3(cre)Bhr/+}$;*YFP*/+ mice and were viewed directly using YFP (yellow fluorescent protein) fluorescence. The testes collected from *Amhr*$^{2tm3(cre)Bhr/+}$; *Ctnnb1*$^{tm1Mmt/+}$ and control mice were photographed by using a Nikon SMZ1500 microscope with an attached Spot camera (Diagnostic Instruments).

Histology Analysis, Immunofluorescence, Immunohistochemistry, and TUNEL staining

Murine testes used in the present study were immersion-fixed in Bouin fluid (for histological analysis) or 4% paraformaldehyde for 10–12 h at 4°C and then transferred to 70% ethanol until processing. The fixed tissues were dehydrated in a graded ethanol series, cleared in xylene, and embedded in paraffin wax. Embedded tissue samples were sectioned (thickness, 5 μm) and then mounted on slides. Hematoxylin-and-eosin and periodic acid-Schiff staining were performed on Bouin-fixed sections using standard histological techniques.

Serial sections of tissues were deparaffinized with xylene and rehydrated with a graded series of ethanol (absolute, 95%, 80% and 50% ethanol, respectively, and distilled water), followed by two washes of 5 min each in PBS containing 0.05% Tween 20 (PBS-T). Tissue sections were then incubated for 10 min in 3% (v/v) hydrogen peroxide in methanol to block endogenous peroxidase activity before immunohistochemistry (IHC). After a wash with PBS-T, antigen retrieval was performed by boiling the tissue sections in 0.01 M citrate buffer (pH 6) for 20 min. Sections were then washed for 5 min in PBS-T and blocked at room temperature for 1 h using 2% normal donkey or goat serum, 2% bovine serum albumin, and 0.1% Triton-X in PBS. Tissues sections were then incubated in humidified chamber overnight at 4°C with primary antibody. Sections were subsequently washed with PBS-T and incubated at room temperature for 1 h with secondary antibody. After a wash with PBS-T, sections for IHC were incubated with ready-to-use streptavidin peroxidase (Lab Vision) for 10 min at room temperature. Afterward, diaminobenzidine (Vector Laboratories) was used to develop color. Sections were counterstained with hematoxylin (IHC) and 4′,6′-diamidino-2-phenylindole (DAPI; immunofluorescence). Both immunofluorescence and IHC images were photographed using a microscope (Nikon Eclipse TE 2000-S) equipped with a Spot digital camera. The primary and secondary antibodies used were as follows: anti-β-catenin (1:250; BD Transduction Laboratories), anti-mouse DDX4 (1:250; Abcam), anti-KIT (1:200; Abcam), anti-GFP (1:200; Abcam), anti-GDNF (1:200; Santa Cruz Biotechnology), anti-AMH (1:100; Santa Cruz Biotechnology), anti-3-hydroxysteroid dehydrogenase (HSD3B1; 1:200; Santa Cruz Biotechnology), vimentin (1:100; Santa Cruz Biotechnology), anti-SOX9 (Chemicon) anti-PCNA (ready to use; Zymed), anti-cyclin D1 (ready to use; Neomarkers), anti-germ cell nuclear antigen 1 (GCNA1; 1:100; Dr. George Enders [23]), AlexaFluor second antibodies (1:500; Invitrogen), and biotinylated donkey anti-mouse or anti-rabbit antibody $F(ab)_2$ (1:1000; Jackson ImmunoResearch Laboratories). TUNEL staining was performed according to instructions provided with the cell death detection kit (Roche).

Counting SOX9-, TUNEL-, and Cyclin D1-Positive Cells

The testicular sections were stained for SOX9, TUNEL, and cyclin D1 as described above. The counting method used in the present study has been described previously and used by Costoya et al. [24]. Briefly, after serial sectioning of mutant and control testes, sections were randomly selected to represent different depths of the whole testes. Sections selected for counting were at least 25 μm apart. SOX9-, TUNEL-, and cyclin D1-positive cells were scored from 40 round tubules of Postnatal Day (PND) 7 and PND 17 testes (n = 3 mice for each genotype). Twenty round tubules from three different independent microscopic fields were counted for PND 35 and adult testes (n = 3 mice for each genotype).

Transfection and Reporter Assays

The luciferase reporter assay was performed as described in our previous studies [25, 26]. Briefly, HEK293 cells (American Type Culture Collection [ATCC]) were plated at a density of 50 000 cells/well in a 24-well plate. The day after plating, cells were transfected with AMH reporter construct [27], GDNF reporter construct [28], and TOPflash construct [29] using Lipofectamine 2000 (Invitrogen). The following day, cells in duplicate wells were treated with indicated concentrations of LiCl and NaCl for 24 h. Results were obtained using the luciferase reporter assay according to the manufacturer's instructions (Promega). Activity was read in a Wallac Victor 3 luminometer (PerkinElmer), and results are shown as an average of three independent experiments. Promoter sequence analyses were performed with MacVector software (MacVector, Inc.).

Statistical Analysis

The unpaired *t*-test was used to test for differences between groups, and $P < 0.05$ was considered to be statistically significant. The statistical analyses were performed using Prism software (GraphPad Software, Inc.).

RESULTS

β-Catenin Expression During Postnatal Testicular Development

To determine where β-catenin might play a role in regulating testicular functions, we first analyzed the expression of β-catenin in testis at various ages by IHC (Fig. 1). We examined testes isolated from mice at PND 7, PND 17, and PND 35 and at adulthood because of the known morphological and functional changes that occur in the juvenile (PND 7 and PND 17) testes as well as those near (PND 35) and at sexual maturity [30]. In PND 7 and PND 17 testes, β-catenin was highly expressed across the width of seminiferous epithelium, specifically in the cytoplasm and membranes of Sertoli cells and also at Sertoli-germ cells junctions (Fig. 1, A and B). In PND 35 and adult testis, β-catenin was highly expressed at basal compartment of seminiferous tubule (Fig. 1, C and D). We also observed weak staining for β-catenin in the nuclei of Sertoli cells at all ages (Fig. 1, A–D, insets), suggesting that active β-catenin signaling is physiologically significant in Sertoli cells. Consistent with previous results [31], very weak or no β-catenin was detected in the interstitial cells of testis (Fig. 1).

Activation of β-Catenin in Sertoli Cells Leads to Abnormal Development of Testis

Because we observed β-catenin expression in Sertoli cells at all stages of postnatal development, we investigated the effect of conditionally expressing an activated allele of β-catenin on Sertoli cells functions and Sertoli-germ cell interactions. *Amhr2*$^{tm3(cre)Bhr/+}$;*Ctnnb1*$^{tm1Mmt/+}$ mice were examined for the effect of dominant stable form of β-catenin, whereas *Ctnnb*$^{1tm1Mmt/+}$ littermates were used as controls. We detected

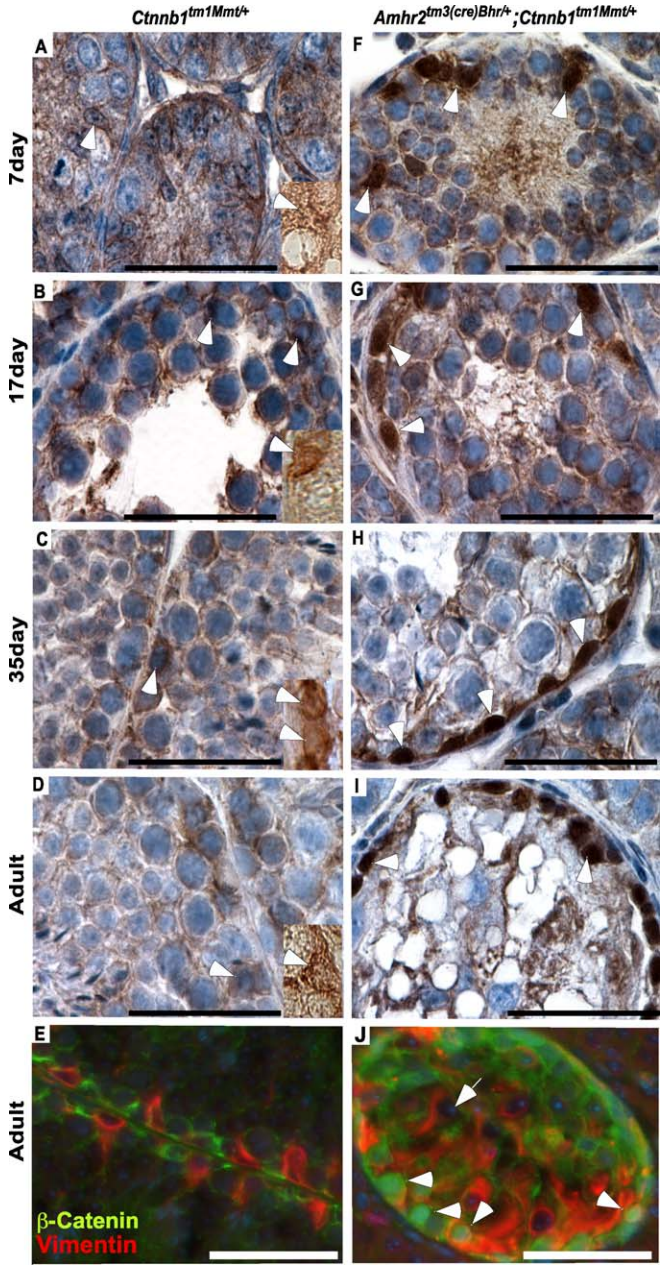

FIG. 1. Localization of β-catenin in testes of both *Amhr2*$^{tm3(cre)Bhr/+}$;*Ctnnb1*$^{flox/+}$ and control postnatal mice. β-Catenin is detected by immunohistochemistry with an anti-β-catenin antibody (brown), and nuclei are counterstained with hematoxylin (blue). In control testes (**A**–**D**), β-catenin is expressed mainly in plasma membrane and cytoplasm of Sertoli cells, but weaker staining is also observed in nuclei of some Sertoli cells (see arrowheads and insets without hematoxylin). In *Amhr2*$^{tm3(cre)Bhr/+}$;*Ctnnb1*$^{tm1Mmt/+}$ testis (**F**–**I**), strong expression of β-catenin is detected in both nuclei (arrowheads) and the cytoplasm of Sertoli cells. **E** and **J**) Colocalization of vimentin (red) and β-catenin (green) in control and mutant adult testes. Arrowheads represent nuclear accumulation of β-catenin in vimentin-positive cells. The arrow points to vimentin-negative cells without nuclear accumulation of β-catenin (arrow). Bar = 50 μm.

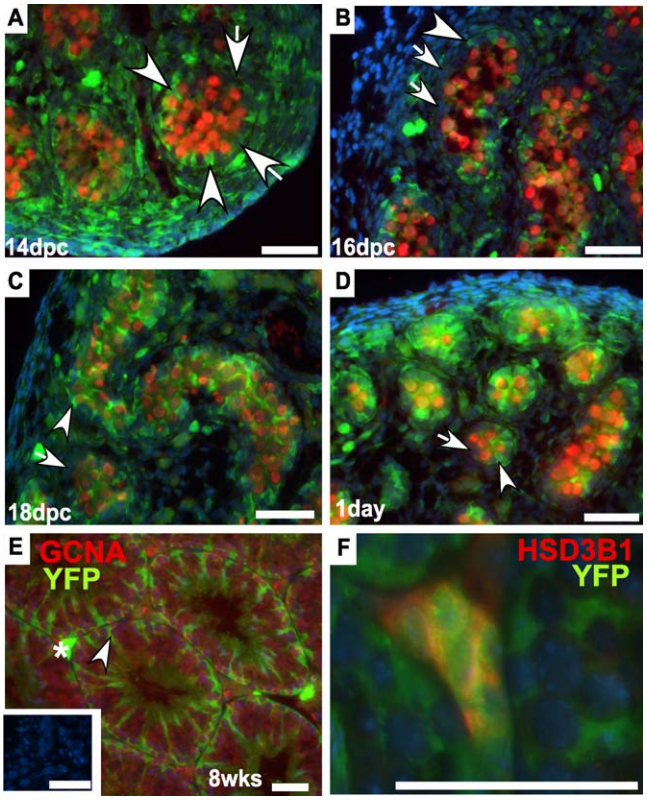

FIG. 2. Expression analysis of a floxed YFP reporter driven by *Amhr2-Cre* in embryonic and postnatal testes. **A**–**D**) In Embryonic Day 14, 16, and 18 as well as Postnatal Day 1 testes, few Sertoli cells were YFP (green) positive (arrowhead), whereas the remaining cells were negative (arrow). YFP expression was also present in interstitial cells and the tunica albuginea. In 8-wk-old testis (**E**) almost all Sertoli cells were YFP positive (arrowhead). YFP positivity was also observed in interstitial cells (asterisk). Inset picture represent the negative controls used for the primary antibodies. **A**–**E**) Germ cells were stained with GCNA (red). **F**) Colocalization of HSD3B1 (red), a Leydig cell marker, and YFP (green). Three animals were examined for each stage of testicular development. Bar = 50 μm.

strong accumulation of β-catenin in the nuclei of a few Sertoli cells in each tubule of *Amhr2*$^{tm3(cre)Bhr/+}$;*Ctnnb1*$^{tm1Mmt/+}$ testes at PND 7 (Fig. 1F), compared to the weak staining for β-catenin detected in nuclei of Sertoli cells in control testis at any age (Fig. 1, A–D). Morphologically, the early PND 7 tubules of the *Amhr2*$^{tm3(cre)Bhr/+}$;*Ctnnb1*$^{tm1Mmt/+}$ testes appeared to be relatively normal when compared to control littermate tubules. As the *Amhr2*$^{tm3(cre)Bhr/+}$;*Ctnnb1*$^{tm1Mmt/+}$ mice aged, more nuclei in each tubule showed strong nuclear β-catenin expression (Fig. 1, G and H), and in adult (age, 12 wk) mice, nearly all Sertoli cell nuclei displayed this pattern (Fig. 1I). To show the activation of β-catenin is limited to the Sertoli cells in seminiferous tubules, we performed experiments to colocalize vimentin, a Sertoli cell marker, with β-catenin (Fig. 1, E and J). We observed that cells with the nuclear accumulation of β-catenin were also positive for vimentin, whereas cells negative for vimentin showed no nuclear accumulation of β-catenin.

Consistent with the findings of Boyer et al. [19], we observed that *Amhr2*$^{tm3(cre)Bhr/+}$;*Ctnnb1*$^{tm1Mmt/+}$ mice had much smaller testes than control littermates and that the weight of adult testes in *Amhr2*$^{tm3(cre)Bhr/+}$;*Ctnnb1*$^{tm1Mmt/+}$ mice was relatively less than the weight in younger mice when compared to control animals, suggesting a progressive decrease in testicular tissue in the mutant animals (Supplemental Fig. S1; all Supplemental Data are available online at www.biolreprod.org). Although mature testes of the *Amhr2*$^{tm3(cre)Bhr/+}$;*Ctnnb1*$^{tm1Mmt/+}$ mice were smaller, early postnatal testes did not appear to be much different histologically from control testes of littermates (Fig. 1, A and B), despite the fact that *Amhr2-Cre* is expressed in embryonic gonads [16]. This suggested three plausible explanations: that *Amhr2-Cre*

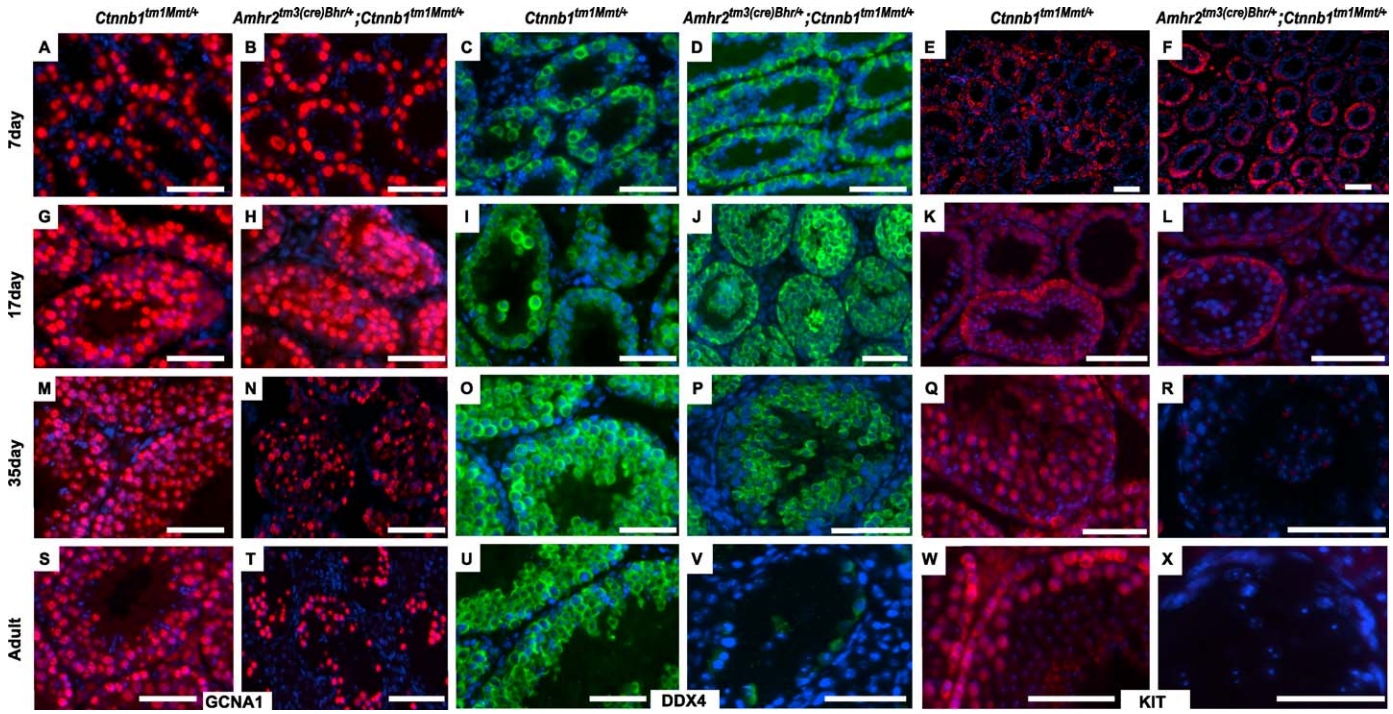

FIG. 3. Stabilization of β-catenin in Sertoli cells causes disruption in the arrangement of germ cells in spermatogenic tubule. Antibodies against GCNA1 (red), DDX4 (green), and KIT (red) were used to detect germ cells in testicular sections by immunofluorescence; nuclei were detected with DAPI (blue). In *Amhr2*$^{tm3(cre)Bhr/+}$;*Ctnnb1*$^{tm1Mmt/+}$ mice testes at Postnatal Day 7, the arrangement of GCNA1-, DDX4-, and KIT-positive cells is similar to that in control littermates (**A**–**F**). In testes at Postnatal Days 17 and 35, GCNA1- and DDX4-positive cells are randomly arranged and also observed in the luminal area of mutant tubules compared to controls (**G**–**J** and **M**–**P**). KIT expression in mutant testes at Postnatal Days 17 and 35 is much weaker than in the controls, particularly in the cells present in the luminal area of mutant testes (**K**, **L**, **Q**, and **R**). In adult *Amhr2*$^{tm3(cre)Bhr/+}$;*Ctnnb1*$^{tm1Mmt/+}$ testes, strongly GCNA1-positive, weakly DDX4-positive, and KIT-negative cells are observed in all the seminiferous tubule compared to controls in which GCNA1-, DDX4-, and KIT-positive cells are present across the width of seminiferous epithelium (**S**–**X**). Bar = 50 μm.

expression was not faithfully recapitulating endogenous *Amhr2* expression, that β-catenin is not normally expressed prenatally in Sertoli cells, or that nuclear β-catenin does not affect early postnatal Sertoli cell functions. Therefore, we investigated the expression of *Amhr2-Cre* at embryonic and in postnatal testes. We generated *Amhr2*$^{tm3(cre)Bhr/+}$;*YFP* mice as described in our previous study [16]. In these mice, we were able to detect *Amhr2-Cre*-driven YFP reporter expression in Sertoli cells of Embryonic Day 14, 16, and 18 as well as 1-day-old and 8-wk-old testes, confirming the expression of *Amhr2-Cre* in both embryonic and postnatal Sertoli cells (Fig. 2, A–E). Interestingly, in both embryonic and PND 1 testes, *Amhr2-Cre*-driven YFP expression was limited to the few Sertoli cells (Fig. 2, A–D). However, all Sertoli cells and some interstitial cells were YFP positive in the adult testis (Fig. 2E). To confirm that *Amhr2-Cre*-driven YFP expression in Leydig cells, we performed colocalization of YFP and HSD3B1 and showed that the YFP-positive cells were also positive for HSD3B1 (Fig. 2F). Our previous study also has shown that the *Amhr2* mRNA is expressed in both embryonic and adult testis [32]. Therefore, although *Amhr2-Cre* expression was detected in prenatal Sertoli cells, we did not observe histologically any defect in embryonic and early postnatal testicular development in *Amhr2*$^{tm3(cre)Bhr/+}$;*Ctnnb1*$^{tm1Mmt/+}$ mice.

Expression of a Stable Form of β-Catenin in Sertoli Cells Disrupts the Germ Cell Microenvironment and Leads to Infertility

As Boyer et al. [19] also showed, no detectable difference was observed histologically between *Amhr2*$^{tm3(cre)Bhr/+}$;*Ctnnb1*$^{tm1Mmt/+}$ and control testes at PND 7 (Supplemental Fig. S2A, a–d). In contrast, in PND 17 mutant testes, we found that lumen formation was inhibited in the vast majority of tubules, which persisted in all *Amhr2*$^{tm3(cre)Bhr/+}$;*Ctnnb1*$^{tm1Mmt/+}$ mice through adulthood (Supplemental Fig. S2A, e–q). At PND 35, round and elongated spermatids are observed in control testes (Supplemental Fig. S2A, j and l) but were absent in mutant testes, except in some tubules where very few round spermatids were observed (Supplemental Fig. S2A, k and m). The presence of round spermatids in the some tubules of mutant testis is consistent with nuclear accumulation of β-catenin in Sertoli of PND 35 mutant testes, where some Sertoli cells still do not show the nuclear accumulation of β-catenin and are able to support germ cell development. In adult *Amhr2*$^{tm3(cre)Bhr/+}$;*Ctnnb1*$^{tm1Mmt/+}$ mice, most of the germ cells are lost, with the exception of a layer of germ cells with Sertoli cells remaining at the base of the seminiferous tubules. We also observed a complete absence of sperm in the tails of the epididymides, further indicating defective spermatogenesis (Supplemental Fig. S2B, a and b). Additionally, multinucleated giant cells were observed in the lumen of many seminiferous tubules of the mutant mice, which likely result from abnormal and incomplete differentiation of germ cells (Supplemental Fig. S2Bc). The identity of these multinucleated cells as germ cells was also confirmed with DDX4 immunostaining (Supplemental Fig. S2Bd).

To determine the identity and the differentiation status of the germ cells that remained in the seminiferous tubules of the mutant mice, we analyzed the expression of known germ cell markers, GCNA1, DDX4 (also known as mouse vasa homolog [mvh]), and the receptor for stem cell factor, KIT, by

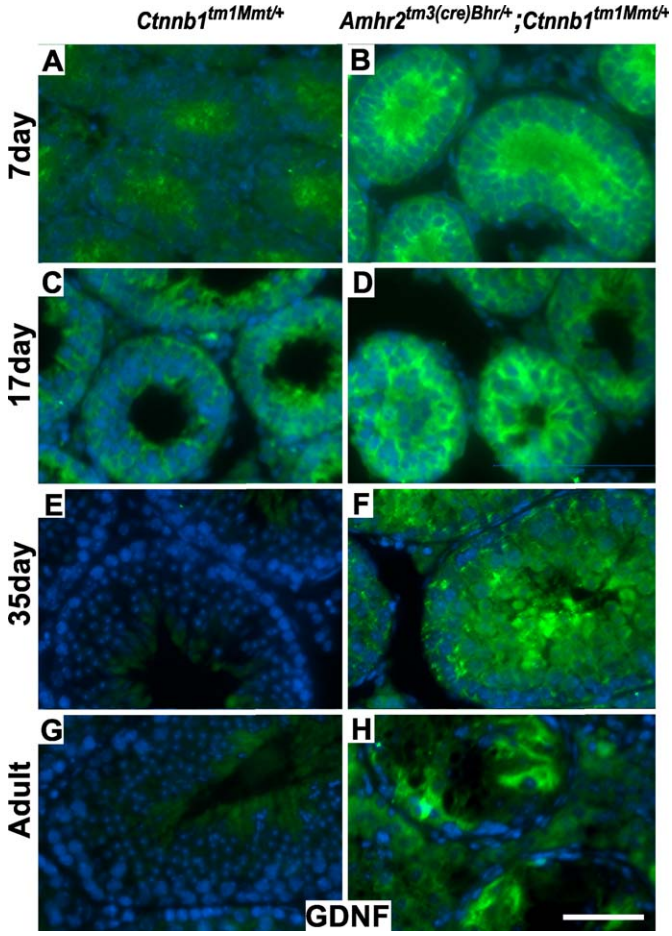

FIG. 4. Sertoli cells of *Amhr2*$^{tm3(cre)Bhr/+}$;*Ctnnb1*$^{tm1Mmt/+}$ mice testes express higher levels of GDNF than littermate control mice. Anti-GDNF was used to detect GDNF by immunofluorescence in testicular sections (green). Nuclei were detected with DAPI (blue). In controls, GDNF protein is detected in Sertoli cells of Postnatal Day 7 (**A**) and Postnatal Day 17 (**C**) mice testes but not in Postnatal Day 35 (**E**) and adult (**G**) mice testes. In *Amhr2*$^{tm3(cre)Bhr/+}$;*Ctnnb1*$^{tm1Mmt/+}$ mice testes, Sertoli cells express GDNF at all the ages examined (**B**, **D**, **F**, and **H**). Bar = 50 μm.

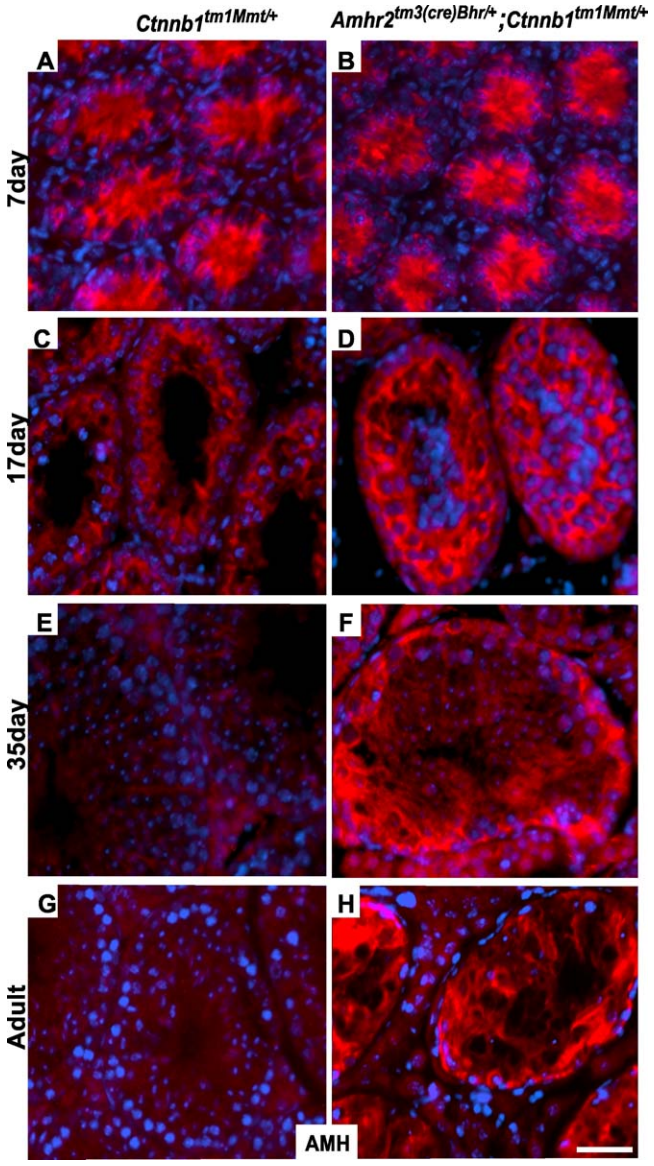

FIG. 5. Sertoli cells with activated β-catenin maintain high levels of AMH expression, an immature Sertoli cell marker. AMH protein was detected in testicular sections by immunofluorescence with an anti-AMH (red), and nuclei were detected with DAPI (blue). In control mice testes, AMH expression level is high at Postnatal Day 7 (**A**), and then a progressive decrease occurs up to adulthood (**C**, **E**, and **G**). In contrast, much higher levels of AMH expression were detected in *Amhr2*$^{tm3(cre)Bhr/+}$;*Ctnnb1*$^{tm1Mmt/+}$ mice testes compared to controls at all ages except Postnatal Day 7, when expression level is similar to that in control (**B**, **D**, **F**, and **H**). Bar = 50 μm.

immunofluorescence. The combination of multiple germ cell markers has been used successfully to identify and isolate different stages of testicular germ cells [34]. For example, in wild-type testes, strong GCNA1 expression is detected in spermatogonia, whereas low levels of expression are detected in spermatocytes and round spermatids [23]. In early postnatal stages of testicular development, gonocytes express mvh; in older but still sexually immature mice, mvh is expressed in germ cell stages from spermatogonia to round spermatids. In adults, the strongest mvh expression is detected at early spermatocyte stages, but lower levels are detected in spermatogonia located at the basal membrane [35, 36]. KIT is a differentiation marker for spermatogonia [37, 38]. In early prepubertal testes, KIT expression is detected on the surface of SSCs. During later stages of testicular development, c-kit is expressed mainly in spermatogonia committed to differentiation [38]. Using an approach involving a combination of these markers, we attempted to identify the status of germ cell development in the *Amhr2*$^{tm3(cre)Bhr/+}$;*Ctnnb1*$^{tm1Mmt/+}$ mice.

In PND 7 testes, the GCNA1-, DDX4-, and KIT-positive cells normally were arranged at the periphery of seminiferous tubules of both *Amhr2*$^{tm3(cre)Bhr/+}$;*Ctnnb1*$^{tm1Mmt/+}$ and control mice (Fig. 3, A–F), which is consistent with the normal histology of mutant testes we had observed at this age. In PND 17 and PND 35 testes, GCNA1- and DDX4-positive cell normally were arranged at the periphery of seminiferous tubules of the control mice (Fig. 3, G, I, M, and O). However, in PND 17 and PND 35 mutant testes, GCNA1- and DDX4-positive cells also were present in the luminal area of tubules (Fig. 3, H, J, N, and P). In control mice, KIT staining was bright and positive (Fig. 3, K and Q); however, KIT expression was very weak or almost absent in the seminiferous tubules of the mutant mice (Fig. 3, L and R). In adult control testes, strongly GCNA1-positive and weakly DDX4-positive cells were present at the circumference of seminiferous tubules, and weakly GCNA1-positive and strongly DDX4-positive cells

were present across the width of seminiferous epithelium (Fig. 3, S and U). Similarly, KIT-positive cells also were present in and around rim of seminiferous tubules (Fig. 3W), consistent with previous observations [39–41]. In adult mutant testes, only strongly GCNA1-positive, weaker DDX4-positive, and KIT-negative cells were observed (Fig. 3, T, V, and X).

Strong GCNA1 and weak DDX4 expression, coupled with absence of KIT expression, reflects the undifferentiated status of spermatogonia. The cluster of germ cells observed in the center of seminiferous tubules of PND 17 and PND 35 *Amhr2*$^{tm3(cre)Bhr/+}$;*Ctnnb1*$^{tm1Mmt/+}$ testes are GCNA1 and DDX4 positive and very weakly KIT positive, suggesting defective differentiation of spermatogonia (Fig. 3, H, J, L, N, P, and R). The germ cells present in seminiferous tubules of *Amhr2*$^{tm3(cre)Bhr/+}$;*Ctnnb1*$^{tm1Mmt/+}$ adult testes are strongly GCNA1 and weakly DDX4 positive (Fig. 3V) as well as KIT negative, confirming their status as undifferentiated spermatogonial cells (Fig. 3, T, V, and X). This phenotype in *Amhr2*$^{tm3(cre)Bhr/+}$;*Ctnnb1*$^{tm1Mmt/+}$ testes is similar to the phenotype of GDNF-overexpressing transgenic mouse testes [4]. In 3-wk-old GDNF transgenic mice testes, spermatogonia accumulate in clusters in the center of tubules, and by 10 wk, most of the germ cells are lost except for a layer of spermatogonia at the periphery of seminiferous tubules [4]. Therefore, we hypothesized that conditional expression of activated β-catenin in Sertoli cells might be either upstream or downstream of GDNF or indirectly affecting the GDNF signaling pathway.

Conditional Activation of β-Catenin in Sertoli Cells Maintains High Expression of GDNF and AMH

The striking similarity in phenotype of *Amhr2*$^{tm3(cre)Bhr/+}$;*Ctnnb1*$^{tm1Mmt/+}$ and GDNF transgenic mice testes led us to investigate expression of GDNF in *Amhr2*$^{tm3(cre)Bhr/+}$;*Ctnnb1*$^{tm1Mmt/+}$ testes. GDNF is thought to be a master regulator of SSC function; when Sertoli cells express GDNF, SSCs proliferate and remain undifferentiated [4]. In control mice, GDNF expression is down-regulated after PND 7 and remains low throughout adulthood (Fig. 4, A–G). In contrast, Sertoli cells of *Amhr2*$^{tm3(cre)Bhr/+}$;*Ctnnb1*$^{tm1Mmt/+}$ testis retained high levels of GDNF expression from PND 7 through adulthood (Fig. 4, B–H).

To further determine the effect of stabilization of β-catenin on the differentiation of Sertoli cells, we analyzed the expression of anti-Müllerian hormone (AMH, also known as Müllerian-inhibiting substance), a classic marker for immature Sertoli cells, in *Amhr2*$^{tm3(cre)Bhr/+}$;*Ctnnb1*$^{tm1Mmt/+}$ and control mice. Normally, AMH expression in Sertoli cells is down-regulated shortly after birth to a very low basal level in adult testes [42]. Similar to GDNF expression in *Amhr2*$^{tm3(cre)Bhr/+}$;*Ctnnb1*$^{tm1Mmt/+}$ testis, AMH expression also is maintained at high levels in Sertoli cells through adulthood in comparison to controls, in which AMH expression is very low or undetectable after PND 17 (Fig. 5, A–H).

Persistent WNT/β-Catenin Signaling in Sertoli Cells Maintains Their Proliferation in Adult Testis

Since we observed expression of AMH and GDNF in Sertoli cells of adult mutant testis, we hypothesized that Sertoli

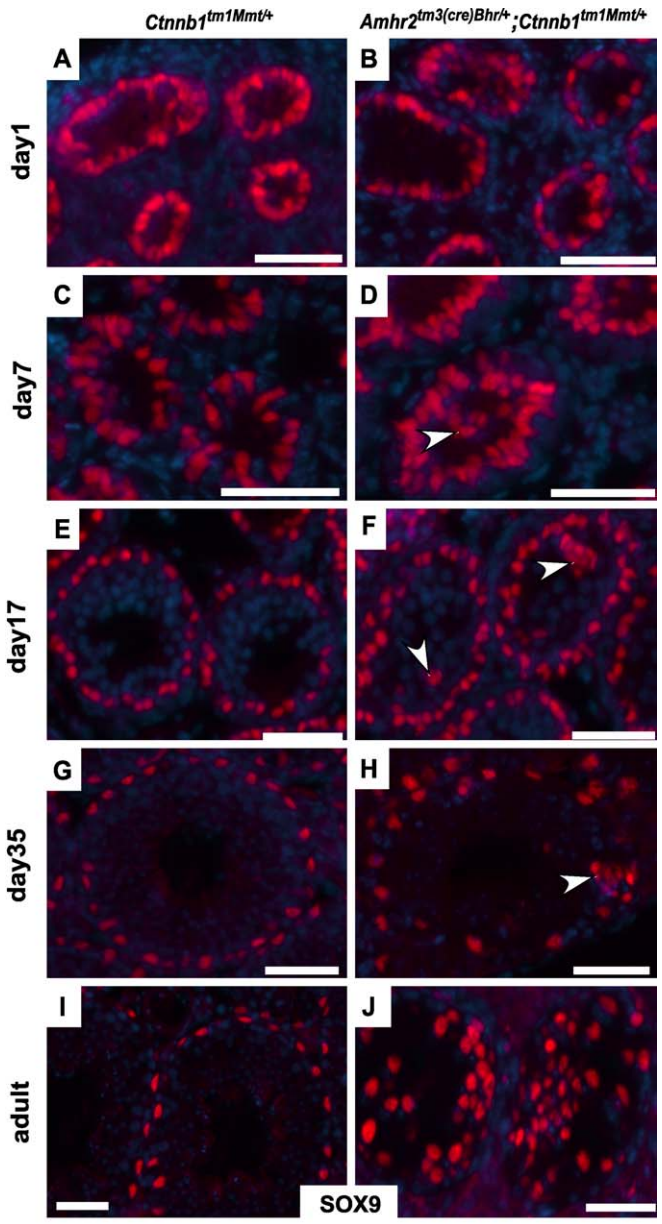

FIG. 6. Localization of SOX9 in *Amhr2*$^{tm3(cre)Bhr/+}$;*Ctnnb1*$^{tm1Mmt/+}$ and control testes. At Postnatal Day 1 (**A** and **B**), no difference was observed between mutant and control testes. At later stages of testicular development (**C–J**), more SOX9-positive Sertoli cells were observed in mutant testes (arrowheads). The graph (**K**) shows mean of number of SOX9-positive cells per tubule in testes of *Amhr2*$^{tm3(cre)Bhr/+}$;*Ctnnb1*$^{tm1Mmt/+}$ and control mice at various ages. Error bars represent the SEM, and an asterisk (*) above a given column indicates a significant difference from control ($P < 0.05$). Bar = 50 μm.

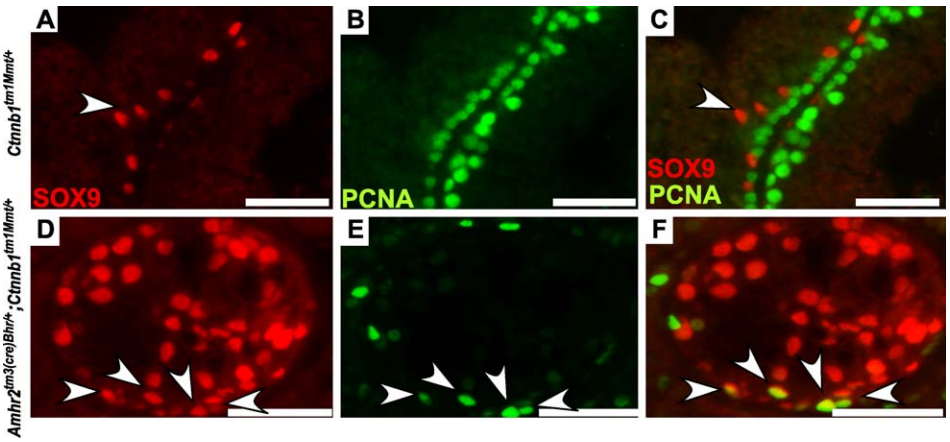

FIG. 7. Activation of β-catenin leads to sustained proliferation of Sertoli cells. We performed coimmunostaining of PCNA (green), a marker of proliferating cells, and SOX9 (red), a Sertoli cell marker to observe the proliferative activity of Sertoli cells in adult testis. **A**) SOX9-positive cells (arrowhead) in adult control testis. **B** and **C**) PCNA-positive (green) in control testis and colocalization of SOX9- and PCNA-positive cells, respectively. All SOX9-positive (arrowhead) cells are negative for PCNA in controls. **D** and **E**) Localization of SOX9 and PCNA in adult mutant testis, respectively. **F**) Coimmunostaining of SOX9 and PCNA in adult mutant testis. Arrowheads represent cells positive for both SOX9 and PCNA. Bar = 50 μm.

cells in mutant testes are relatively immature and proliferating. To assess the number of Sertoli cells between control and mutant testis, we analyzed the expression of SOX9, a Sertoli cell marker. We observed more SOX9-positive cells at all ages in mutant testes compared to control except at PND 1, when no difference was observed (Fig. 6, A–J). To quantify the number of Sertoli cells in control and mutant testis, we performed a SOX9-positive cell count and observed a significantly higher number of Sertoli cells in mutant testes than control at all stages except PND 1 (Fig. 6K). Additionally, colocalization of SOX9 and PCNA indicated no proliferating Sertoli cells in control adult testis (Fig. 7, A–C). In contrast, proliferating Sertoli cells were observed in mutant testis (Fig. 7, D–F, arrowheads), suggesting that the increase in the number of Sertoli cells in mutant testis is because of continued proliferation of Sertoli cells. Collectively, these findings indicate that the Sertoli cells in mutant testis are maintained in an immature state.

Activation of β-Catenin in Sertoli Cells Leads to Decreased Proliferation and Increased Apoptosis of Germ Cells

To determine whether accumulation of undifferentiated spermatogonia in tubules of *Amhr2*$^{tm3(cre)Bhr/+}$;*Ctnnb1*$^{tm1Mmt/+}$ testes is caused by a spermatogonial differentiation defect or by hyperproliferation of spermatogonia, we performed expression analysis of cyclin D1, a marker for mitotic spermatogonia [24]. Normally, mitotically active germ cells are located at or near the basal compartment, whereas meiotic germ cells are present in the more adluminal compartment of the seminiferous tubule. However, in the mutant mice, we observed mitotically active germ cells in the lumen (Fig. 8). To assay the number of cyclin D1-positive cells in *Amhr2*$^{tm3(cre)Bhr/+}$;*Ctnnb1*$^{tm1Mmt/+}$ and control testes, we scored cyclin D1-positive cells. The number of mitotic spermatogonia, from PND 17 to adulthood, in testis of *Amhr2*$^{tm3(cre)Bhr/+}$;*Ctnnb1*$^{tm1Mmt/+}$ was significantly decreased compared to that in littermate controls (Fig. 8), indicating that a differentiation defect, not hyperproliferation, of spermatogonia causes accumulation of germ cells in *Amhr2*$^{tm3(cre)Bhr/+}$;*Ctnnb1*$^{tm1Mmt/+}$ testis.

A block in spermatogonial differentiation or accumulation of spermatogonia in seminiferous tubules has been shown to induce germ cell death in juvenile spermatogonial depletion (*Utp14b*) and *Bax* knockout mice [43, 44] as well as in *Bcl2l1* or *Bcl2* transgenic and GDNF-overexpressing mice testes [4, 43–45]. This led us to hypothesize that the germ cell loss we observed in *Amhr2*$^{tm3(cre)Bhr/+}$;*Ctnnb1*$^{tm1Mmt/+}$ adult testis was the result of increased apoptosis caused by accumulation of spermatogonia undergoing defective spermatogenesis. To test this hypothesis, we performed TUNEL analyses to assess the degree of cell death in *Amhr2*$^{tm3(cre)Bhr/+}$;*Ctnnb1*$^{tm1Mmt/+}$ and control testes. To estimate the total number of apoptotic cells, we used the counting method described above for estimating cyclin D1-positive cells. We observed a significantly higher average number of TUNEL-positive cells in *Amhr2*$^{tm3(cre)Bhr/+}$;*Ctnnb1*$^{tm1Mmt/+}$ than in control testis (Fig. 9) at all ages that we examined. Additionally, we did not observe any TUNEL-positive cells in the center of the mutant tubules (Fig. 9F, arrowhead), suggesting that the cyclin D1-positive cells observed in the center of the mutant tubules are not dead cells. Collectively, these findings support the hypothesis that defective differentiation of spermatogonia leads to their accumulation in tubules and increased apoptosis.

WNT/β-Catenin Directly Induces GDNF and AMH Expression

Because constitutive activation of β-catenin signaling leads to persistent high expression of GDNF and AMH in Sertoli cells, we examined whether β-catenin regulated both of these genes at the transcriptional level. Primary Sertoli cells are not easily transfected, and the TOPflash-optimized β-catenin luciferase reporter [29] does not respond to the GSK3B inhibitor, LiCl, in the TM4 Sertoli cell line (data not shown). Therefore, we used HEK293 cells, which are transfectable and have an intact WNT/β-catenin signaling system, to study transcriptional regulation of the *Amh* and *Gdnf* promoters. We observed a twofold increase in *Amh* promoter activity with 10 mM LiCl compared to control (10 mM NaCl treatment), but this was less than similarly treated cells transfected with the control TOPflash, β-catenin luciferase promoter (Fig. 10A). On the basis of these results and our previous observations described above, we hypothesized that continued AMH expression in Sertoli cells may be responsible, at least in part, for the mutant phenotype and that deletion of *Amh* or *Amhr2* would be able to rescue the phenotype observed in *Amhr2*$^{tm3(cre)Bhr/+}$;*Ctnnb1*$^{tm1Mmt/+}$ mice testes. For this reason, we developed *Amhr2*$^{tm3(cre)Bhr/Amhr2tm3(cre)Bhr}$;*Ctnnb1*$^{tm1Mmt/+}$ mice, in which activated β-catenin is expressed on an *Amhr2* receptor-null background. We did not observe a difference in the testicular phenotype of 7-wk-old *Amhr*$^{2tm3(cre)Bhr/Amhr2tm3(cre)Bhr}$;*Ctnnb1*$^{tm1Mmt/+}$ (Fig. 10B) and *Amhr2*$^{tm3(cre)Bhr/+}$;*Ctnnb1*$^{tm1Mmt/+}$ testis, indicating that continued expression of *Amh* in Sertoli cells in response to constitutive expression of activated β-catenin does not play an essential role in the *Amhr2*$^{tm3(cre)Bhr/+}$;*Ctnnb1*$^{tm1Mmt/+}$ testicular phenotype. We also observed that activation of β-catenin by treatment with 10 mM

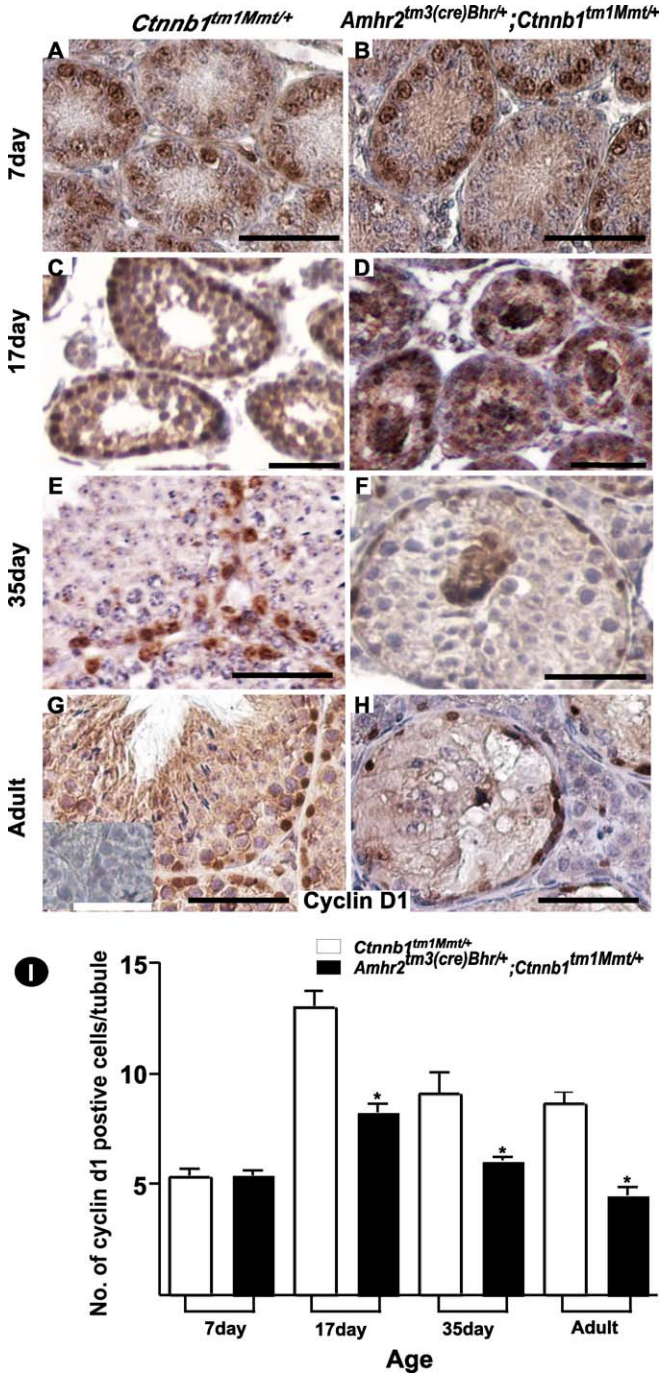

FIG. 8. Representative testicular sections from *Amhr2*$^{tm3(cre)Bhr/+}$;*Ctnnb1*$^{tm1Mmt/+}$ (**B**, **D**, **F**, and **H**) and control mice (**A**, **C**, **E**, and **G**) stained with cyclin D1, a marker for mitotic spermatogonia. Anti-cyclin D1 was used to detect cyclin D1 by immunohistochemistry (brown); nuclei are counterstained with hematoxylin. In Postnatal Day 7 testes, cyclin D1-positive cells are similarly arranged in control and mutant testes (**A** and **B**). In mutant testes at Postnatal Days 17 and 35 and adulthood, cyclin D1-positive cells are also present in the center of the seminiferous tubules (arrowheads), whereas in controls, positive cells are only present at the periphery of tubules (**C**–**H**). Inset in **G** represent the control with no primary antibody. The graph (**I**) shows the mean number of cyclin D1-positive cells per tubule in testes of *Amhr2*$^{tm3(cre)Bhr/+}$;*Ctnnb1*$^{tm1Mmt/+}$ and control mice at various ages. At all ages, fewer cyclin D1-positive spermatogonia are observed in *Amhr2*$^{tm3(cre)Bhr/+}$;*Ctnnb1*$^{tm1Mmt/+}$ mice than in control mice except for Postnatal Day 7 testes, in which the number of cyclin D1-positive cells are similar for both groups. Three animals were analyzed for each time points and genotype. Error bars represent the SEM, and an asterisk (*) above a given column indicates a significant difference from control ($P < 0.05$). Bar = 50 μm.

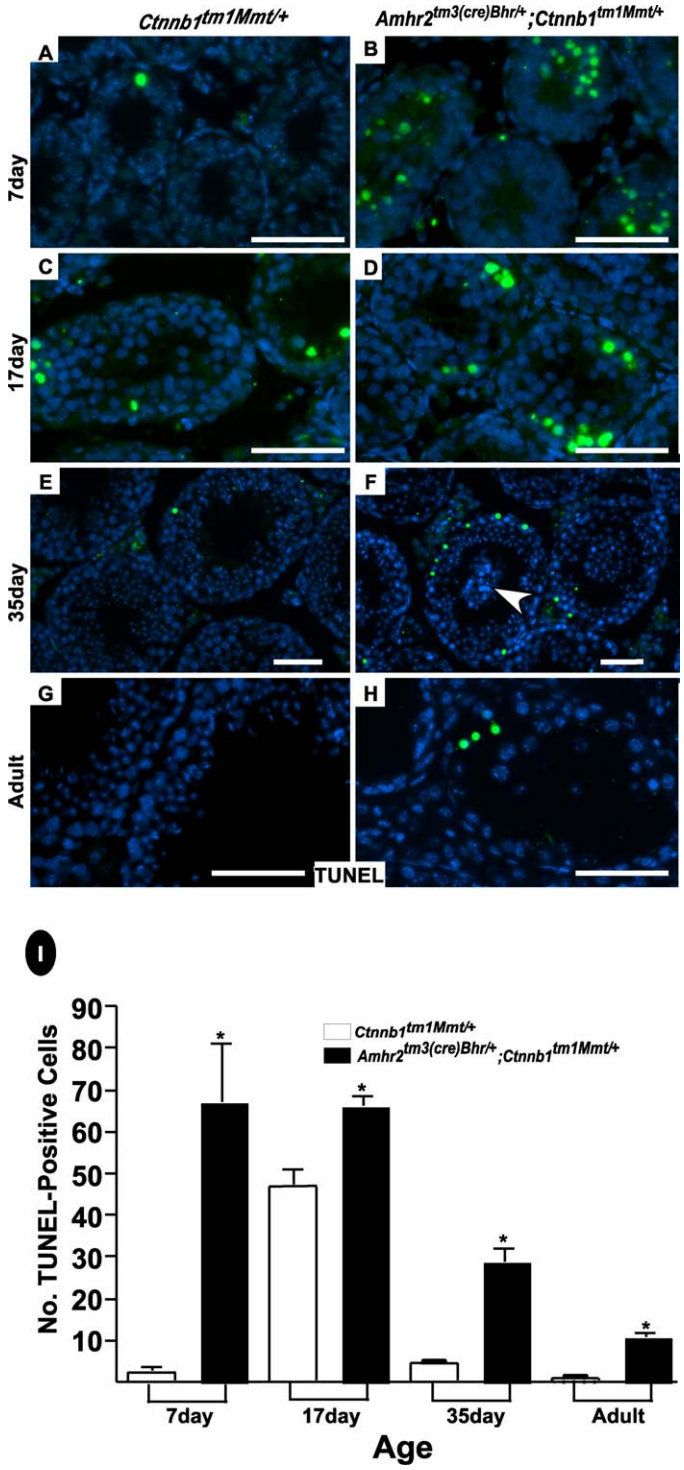

FIG. 9. Increased apoptosis in testicular sections from *Amhr2*$^{tm3(cre)Bhr/+}$;*Ctnnb1*$^{tm1Mmt/+}$ mice. Apoptotic cells (green) were observed by the TUNEL assay, which detects fragmented DNA. Control mice (**A**, **C**, **E**, and **G**) have fewer TUNEL-positive cells at all the ages compared to the mutant mice (**B**, **D**, **F**, and **H**). The graph (**I**) shows the mean number of apoptotic cells in testes of *Amhr2*$^{tm3(cre)Bhr/+}$;*Ctnnb1*$^{tm1Mmt/+}$ and control mice. At all the ages, a significantly higher number of TUNEL-positive cells is present in mutant testes than in controls. Forty tubules per testis per animal for each genotype were scored for each of first two time points (Postnatal Days 7 and 17), whereas 20 or more tubules per testis per animal from three different microscopic fields were scored for Postnatal Day 35 and adult testis. Three animals were analyzed for each time point and genotype. The arrowhead in **F** represents the cells present in the center of the tubules in mutant testes that are TUNEL negative. Error bars represent the SEM, and an asterisk (*) above a given column indicates a significant difference from control ($P < 0.05$). Bar = 50 μm.

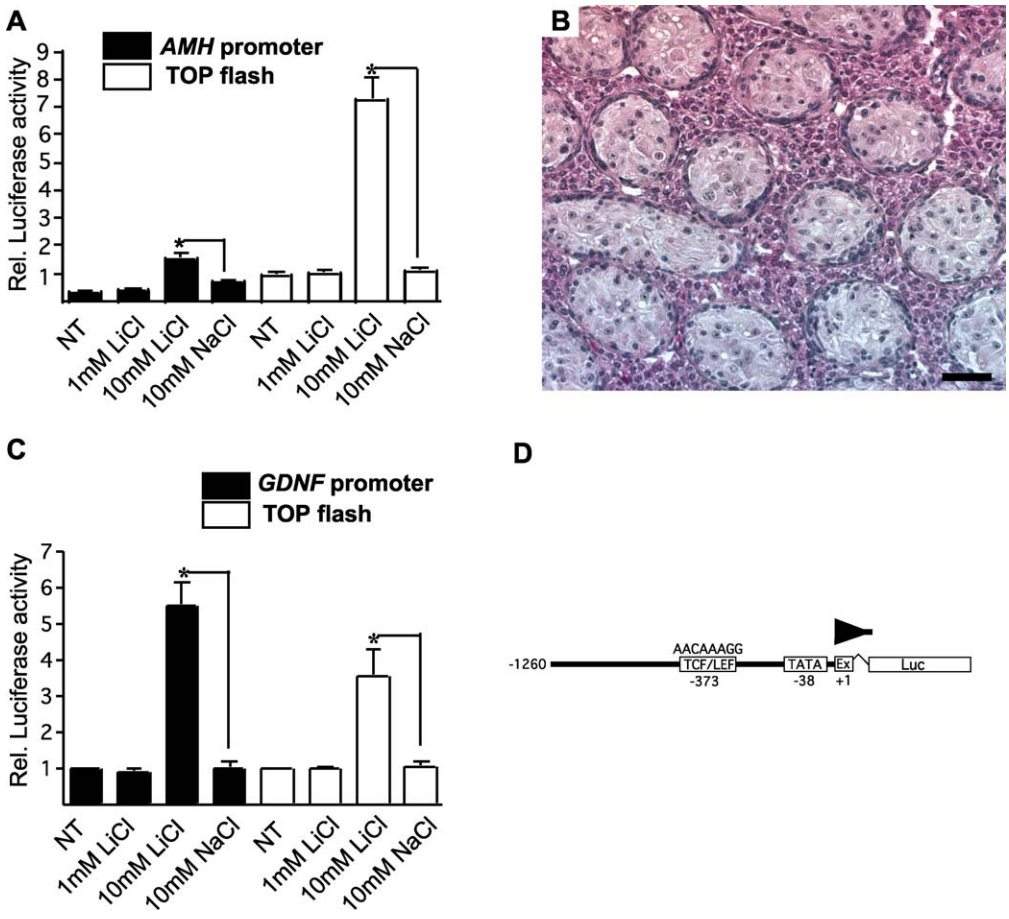

FIG. 10. WNT/β-catenin signaling directly regulates *Amh* and *Gdnf* promoter activity. **A**) HEK293 cells were transfected with either the rat *Amh* or the TOPflash luciferase reporters and treated as indicated. **B**) Hematoxylin and eosin-stained section of mouse testis shows that conditional ablation of AMH signaling does not rescue mutant phenotype observed in $Amhr2^{tm3(cre)Bhr/+}$;$Ctnnb1^{tm1Mmt/+}$testes. **C**) HEK293 cells were transfected with either the mouse *Gdnf* or the TOPflash luciferase reporters and treated as indicated. **D**) Schematic presentation of GDNF proximal promoter showing the consensus TCF/LEF binding site. Luciferase results in **A** and **B** are representative of mean values of three independent experiments performed in duplicate. Error bars represent the SEM, and an asterisk (*) above a given column indicates a significant difference from control ($P < 0.05$). Bar = 50 μm.

LiCl caused a fivefold increase in *Gdnf* promoter activity (Fig. 10C), which was greater than the induction observed with the optimized TOPflash reporter. Sequence analyses of the proximal *Gdnf* promoter showed a perfect match to the *Tcf7* consensus binding site [46] (Fig. 10D). We also observed several core *Tcf7*/*Lef1* consensus [47] sites in both the *Gdnf* and *Amh* promoters (data not shown). Collectively, these results suggest that GDNF expression is directly regulated by β-catenin.

DISCUSSION

We have shown that constitutively activated WNT/β-catenin signaling in Sertoli cells inhibits their differentiation, as demonstrated by the continued proliferation and expression of the juvenile markers GDNF and AMH. Although the mutant Sertoli cells can still support SSC survival, they are no longer capable of supporting spermatogenesis, as evidenced by the increased germ cell apoptosis we observed. Various components of WNT pathways have been shown previously to play an essential role during spermatogenesis in mice. For example, defects in Sertoli cell differentiation have been observed in *Wnt4*-deleted mice, and deletion of canonical WNT signaling antagonist, naked cuticle 1 (NKD1), leads to defective formation of elongated spermatid [48, 49]. In seminiferous epithelium, WNT1 and disheveled 1 are expressed in round germ cells [48, 50], whereas the WNT antagonists, dickkopf-like 1 and NKD1, are expressed mainly in elongated spermatids [48, 51]. This opposing distribution pattern of WNT signaling agonists and antagonists indicates that a delicate balance of canonical WNT signaling is required for the proper differentiation of germ cells.

Our data suggest one mechanism that might be involved in causing defective spermatogenesis in the mutants is the continued proliferation of Sertoli cells. In rodent seminiferous epithelium, each single Sertoli cell is associated with 30–50 germ cells [52]. Deviation from this ratio is symptomatic of defective spermatogenesis. Apoptosis is physiologically required for the maintenance of an optimal ratio of spermatogonia to Sertoli cells in seminiferous epithelium; excessive apoptosis, however, leads to germ cell death and infertility [45, 53]. At 2–3 wk of age, large numbers of spermatogonia and spermatocytes undergo apoptosis in mice testes, possibly to maintain normal germ cell density in the seminiferous epithelium. In adult mice testes, early spermatogonia regularly undergo apoptosis to maintain the proper ratio between Sertoli and germ cells. The molecular players involved in controlling apoptosis in the testes of young animals are different from the apoptotic pathway involved in regulation of germ cell death in adult testes. The identities and origins of the stimuli that trigger germ cell apoptosis in prepubertal and adult testes are largely unknown, but some of the proteins involved in classical apoptosis are known to be involved here as well. Overexpres-

sion of BCL2 and BCL2L1 and deletion of BAX block this early wave of apoptosis and cause excess accumulation of spermatogonia. Subsequently, this increase in the number of spermatogonia stimulates the adult germ cell apoptotic pathway, leading to infertility in adult mice [44, 45, 54]. These findings further underline the importance of cell death pathways in controlling the germ cell population in mice testes. The spermatogonial differentiation defect observed in juvenile spermatogonial depletion (*Utp14b*) and *Gdnf* transgenic mice testes are accompanied by increase germ cell apoptosis [4, 43]. The increased apoptosis observed in these mouse models might be caused by excess accumulation of spermatogonia, which activates apoptotic pathways required to control germ cell density in seminiferous epithelium. In the present study, we observed more TUNEL-positive germ cells in *Amhr2*$^{tm3(cre)Bhr/+}$;*Ctnnb1*$^{tm1Mmt/+}$ testes than in control testes, suggesting that disrupted spermatogonial differentiation leads to their accumulation in seminiferous tubules, which might subsequently activate the apoptotic pathway required to control the normal germ cell density, resulting in increased germ cell death.

Another mechanism that might be contributing to the germ cell apoptosis we observed is the continued expression of GDNF, which is secreted by immature Sertoli cells and has been shown to regulate SSC functions in both in vivo and in vitro conditions [4, 55]. The deletion of GDNF in mice leads to depletion of the SSC reserve and disrupted spermatogenesis [4]. Overexpression of GDNF leads to clustering of undifferentiated spermatogonia in the seminiferous tubule at 3 wk of age, and only undifferentiated spermatogonia with Sertoli cells remain in adult testes [4]. We show that GDNF expression is both higher and maintained throughout adulthood in the Sertoli cells of *Amhr2*$^{tm3(cre)Bhr/+}$;*Ctnnb1*$^{tm1Mmt/+}$ mice testes compared to controls. Another possible effector inhibiting spermatogenesis is the high level of AMH expression in adult mutant Sertoli cells. Abrogation of AMH signaling has no known effect on spermatogenesis in either ligand or receptor knockout studies [56, 57]. However, overexpression of AMH under the control of the metallothionein promoter leads to severe defects in testicular morphology and spermatogenesis [58], suggesting that the postpubertal expression of AMH that we observed in *Amhr2*$^{tm3(cre)Bhr/+}$;*Ctnnb1*$^{tm1Mmt/+}$ mice testes might also play a role in disrupting spermatogenesis in these mice. Interestingly, we have shown evidence that activation of WNT/β-catenin signaling increased both GDNF and AMH promoter activity, suggesting that WNT/β-catenin is directly regulating their expression. However, of the two, only GDNF remains a candidate for the infertility phenotype, because abrogating AMH signaling in the *Amhr2*$^{tm3(cre)Bhr/Amhr2tm3(cre)Bhr}$;*Ctnnb1*$^{tm1Mmt/+}$ mice did not prevent development of the mutant phenotype. Definitive identification of GDNF as the proximal cause of the *Amhr2*$^{tm3(cre)Bhr/+}$;*Ctnnb1*$^{tm1Mmt/+}$ mutant phenotype in the testis will require constitutive activation of β-catenin in mice combined with postnatal conditional deletion of GDNF signaling, because two functional alleles of GDNF are needed for normal testicular differentiation [4].

Amhr2-Cre is also expressed in interstitial cells of the testis, and any confounding effects from that expression might be of concern. However, we observed no phenotypic defect in Leydig cells when comparing control and mutant mice testes. In adult mutant testis, it appears that Leydig cell hyperplasia does occur. However, at this stage, mutant testes are much smaller than control testes, and their weight is one fifth that of the control testes, suggesting the apparent increase in Leydig cells numbers in any given section is caused by the decrease in total volume of the adult mutant testis. Similar observations were also made in other mouse models with defective Sertoli and/or Sertoli-germ functions [4, 33]. Additionally, we did not observe a difference in HSD3B1 staining, a Leydig cell marker, between mutant and control testis (Supplemental Fig. S3). Also, Boyer et al. [19] showed that serum testosterone was not significantly different from the level in control mice, suggesting that expression of a constitutively activated form of β-catenin in Leydig cells probably does not contribute to the testicular phenotype we have observed.

In summary, we have shown that constitutive activation of WNT/β-catenin in Sertoli cells compromises the differentiation or maturation of Sertoli cells, leading to disruption of the germ cell microenvironment and, subsequently, to infertility.

ACKNOWLEDGMENTS

We would like to thank Dr. Richard Behringer for providing us with the *Amhr2*$^{tm3(cre)Bhr}$ mice and Drs. Dorri Woods, Nelson Arango, Yin Xia, and James R. McFarlane for reviewing an early version of the manuscript.

REFERENCES

1. de Rooij DG, Russell LD. All you wanted to know about spermatogonia but were afraid to ask. J Androl 2000; 21:776–798.
2. Shinohara T, Orwig KE, Avarbock MR, Brinster RL. Restoration of spermatogenesis in infertile mice by Sertoli cell transplantation. Biol Reprod 2003; 68:1064–1071.
3. Brinster RL, Zimmermann JW. Spermatogenesis following male germ-cell transplantation. Proc Natl Acad Sci U S A 1994; 91:11298–11302.
4. Meng X, Lindahl M, Hyvonen ME, Parvinen M, de Rooij DG, Hess MW, Raatikainen-Ahokas A, Sainio K, Rauvala H, Lakso M, Pichel JG, Westphal H, et al. Regulation of cell fate decision of undifferentiated spermatogonia by GDNF. Science 2000; 287:1489–1493.
5. Kanatsu-Shinohara M, Miki H, Inoue K, Ogonuki N, Toyokuni S, Ogura A, Shinohara T. Germline niche transplantation restores fertility in infertile mice. Hum Reprod 2005; 20:2376–2382.
6. Chen C, Ouyang W, Grigura V, Zhou Q, Carnes K, Lim H, Zhao GQ, Arber S, Kurpios N, Murphy TL, Cheng AM, Hassell JA, et al. ERM is required for transcriptional control of the spermatogonial stem cell niche. Nature 2005; 436:1030–1034.
7. Wodarz A, Nusse R. Mechanisms of Wnt signaling in development. Annu Rev Cell Dev Biol 1998; 14:59–88.
8. Nusse R. Wnt signaling and stem cell control. Cell Res 2008; 18:523–527.
9. Clevers H. Wnt/beta-catenin signaling in development and disease. Cell 2006; 127:469–480.
10. Siegfried E, Wilder EL, Perrimon N. Components of wingless signaling in *Drosophila*. Nature 1994; 367:76–80.
11. McMahon AP, Moon RT. Ectopic expression of the proto-oncogene int-1 in *Xenopus* embryos leads to duplication of the embryonic axis. Cell 1989; 58:1075–1084.
12. Yoshikawa Y, Fujimori T, McMahon AP, Takada S. Evidence that absence of Wnt-3a signaling promotes neuralization instead of paraxial mesoderm development in the mouse. Dev Biol 1997; 183:234–242.
13. Stark K, Vainio S, Vassileva G, McMahon AP. Epithelial transformation of metanephric mesenchyme in the developing kidney regulated by Wnt-4. Nature 1994; 372:679–683.
14. Yamaguchi TP, Bradley A, McMahon AP, Jones S. A Wnt5a pathway underlies outgrowth of multiple structures in the vertebrate embryo. Development 1999; 126:1211–1223.
15. Miller C, Sassoon DA. Wnt-7a maintains appropriate uterine patterning during the development of the mouse female reproductive tract. Development 1998; 125:3201–3211.
16. Arango NA, Szotek PP, Manganaro TF, Oliva E, Donahoe PK, Teixeira J. Conditional deletion of beta-catenin in the mesenchyme of the developing mouse uterus results in a switch to adipogenesis in the myometrium. Dev Biol 2005; 288:276–283.
17. Nelson WJ, Nusse R. Convergence of Wnt, beta-catenin, and cadherin pathways. Science 2004; 303:1483–1487.
18. Golestaneh N, Beauchamp E, Fallen S, Kokkinaki M, Uren A, Dym M. Wnt signaling promotes proliferation and stemness regulation of spermatogonial stem/progenitor cells. Reproduction 2009; 138:151–162.
19. Boyer A, Hermo L, Paquet M, Robaire B, Boerboom D. Seminiferous tubule degeneration and infertility in mice with sustained activation of WNT/CTNNB1 signaling in Sertoli cells. Biol Reprod 2008; 79:475–485.
20. Jamin SP, Arango NA, Mishina Y, Hanks MC, Behringer RR.

Requirement of Bmpr1a for Mullerian duct regression during male sexual development. Nat Genet 2002; 32:408–410.
21. Harada N, Tamai Y, Ishikawa T, Sauer B, Takaku K, Oshima M, Taketo MM. Intestinal polyposis in mice with a dominant stable mutation of the beta-catenin gene. EMBO J 1999; 18:5931–5942.
22. Srinivas S, Watanabe T, Lin CS, William CM, Tanabe Y, Jessell TM, Costantini F. Cre reporter strains produced by targeted insertion of EYFP and ECFP into the ROSA26 locus. BMC Dev Biol 2001; 1:4.
23. Enders GC, May JJ II. Developmentally regulated expression of a mouse germ cell nuclear antigen examined from embryonic day 11 to adult in male and female mice. Dev Biol 1994; 163:331–340.
24. Costoya JA, Hobbs RM, Barna M, Cattoretti G, Manova K, Sukhwani M, Orwig KE, Wolgemuth DJ, Pandolfi PP. Essential role of Plzf in maintenance of spermatogonial stem cells. Nat Genet 2004; 36:653–659.
25. Renlund N, O'Neill FH, Zhang L, Sidis Y, Teixeira J. Activin receptor-like kinase-2 inhibits activin signaling by blocking the binding of activin to its type II receptor. J Endocrinol 2007; 195:95–103.
26. Renlund N, Pieretti-Vanmarcke R, O'Neill FH, Zhang L, Donahoe PK, Teixeira J. c-Jun N-terminal kinase inhibitor II (SP600125) activates Mullerian-inhibiting substance type II receptor-mediated signal transduction. Endocrinology 2008; 149:108–115.
27. Watanabe K, Clarke TR, Lane AH, Wang X, Donahoe PK. Endogenous expression of Mullerian-inhibiting substance in early postnatal rat Sertoli cells requires multiple steroidogenic factor-1 and GATA-4-binding sites. Proc Natl Acad Sci U S A 2000; 97:1624–1629.
28. Tanaka M, Ito S, Matsushita N, Mori N, Kiuchi K. Promoter analysis and characteristics of the 5′-untranslated region of the mouse glial cell line-derived neurotrophic factor gene. Brain Res Mol Brain Res 2000; 85:91–102.
29. Veeman MT, Slusarski DC, Kaykas A, Louie SH, Moon RT. Zebrafish prickle, a modulator of noncanonical Wnt/Fz signaling, regulates gastrulation movements. Curr Biol 2003; 13:680–685.
30. Setchell BP. The Mammalian Testis. Ithaca, NY: Cornell University Press; 1978.
31. Byers SW, Sujarit S, Jegou B, Butz S, Hoschutzky H, Herrenknecht K, MacCalman C, Blaschuk OW. Cadherins and cadherin-associated molecules in the developing and maturing rat testis. Endocrinology 1994; 134:630–639.
32. Teixeira J, He WW, Shah PC, Morikawa N, Lee MM, Catlin EA, Hudson PL, Wing J, Maclaughlin DT, Donahoe PK. Developmental expression of a candidate Mullerian-inhibiting substance type II receptor. Endocrinology 1996; 137:160–165.
33. Papaioannou MD, Pitetti JL, Ro S, Park C, Aubry F, Schaad O, Vejnar CE, Kuhne F, Descombes P, Zdobnov EM, McManus MT, Guillou F, et al. Sertoli cell Dicer is essential for spermatogenesis in mice. Dev Biol 2009; 326:250–259.
34. Oatley JM, Brinster RL. Regulation of spermatogonial stem cell self-renewal in mammals. Annu Rev Cell Dev Biol 2008; 24:263–286.
35. Tanaka SS, Toyooka Y, Akasu R, Katoh-Fukui Y, Nakahara Y, Suzuki R, Yokoyama M, Noce T. The mouse homolog of *Drosophila* Vasa is required for the development of male germ cells. Genes Dev 2000; 14: 841–853.
36. Toyooka Y, Tsunekawa N, Takahashi Y, Matsui Y, Satoh M, Noce T. Expression and intracellular localization of mouse vasa-homologue protein during germ cell development. Mech Dev 2000; 93:139–149.
37. Ohbo K, Yoshida S, Ohmura M, Ohneda O, Ogawa T, Tsuchiya H, Kuwana T, Kehler J, Abe K, Scholer HR, Suda T. Identification and characterization of stem cells in prepubertal spermatogenesis in mice small star, filled. Dev Biol 2003; 258:209–225.
38. Schrans-Stassen BH, van de Kant HJ, de Rooij DG, van Pelt AM. Differential expression of c-kit in mouse undifferentiated and differentiating type A spermatogonia. Endocrinology 1999; 140:5894–5900.
39. Prabhu SM, Meistrich ML, McLaughlin EA, Roman SD, Warne S, Mendis S, Itman C, Loveland KL. Expression of c-Kit receptor mRNA and protein in the developing, adult and irradiated rodent testis. Reproduction 2006; 131:489–499.
40. Yoshinaga K, Nishikawa S, Ogawa M, Hayashi S, Kunisada T, Fujimoto T. Role of c-kit in mouse spermatogenesis: identification of spermatogonia as a specific site of c-kit expression and function. Development 1991; 113: 689–699.
41. Manova K, Nocka K, Besmer P, Bachvarova RF. Gonadal expression of c-kit encoded at the W locus of the mouse. Development 1990; 110:1057–1069.
42. Teixeira J, Maheswaran S, Donahoe PK. Mullerian-inhibiting substance: an instructive developmental hormone with diagnostic and possible therapeutic applications. Endocr Rev 2001; 22:657–674.
43. Shetty G, Shao SH, Weng CC. p53-dependent apoptosis in the inhibition of spermatogonial differentiation in juvenile spermatogonial depletion (Utp14bjsd) mice. Endocrinology 2008; 149:2773–2781.
44. Knudson CM, Tung KS, Tourtellotte WG, Brown GA, Korsmeyer SJ. Bax-deficient mice with lymphoid hyperplasia and male germ cell death. Science 1995; 270:96–99.
45. Rodriguez I, Ody C, Araki K, Garcia I, Vassalli P. An early and massive wave of germinal cell apoptosis is required for the development of functional spermatogenesis. EMBO J 1997; 16:2262–2270.
46. Oosterwegel M, van de Wetering M, Dooijes D, Klomp L, Winoto A, Georgopoulos K, Meijlink F, Clevers H. Cloning of murine TCF-1, a T cell-specific transcription factor interacting with functional motifs in the CD3-epsilon and T cell receptor alpha enhancers. J Exp Med 1991; 173: 1133–1142.
47. Giese K, Amsterdam A, Grosschedl R. DNA-binding properties of the HMG domain of the lymphoid-specific transcriptional regulator LEF-1. Genes Dev 1991; 5:2567–2578.
48. Li Q, Ishikawa TO, Miyoshi H, Oshima M, Taketo MM. A targeted mutation of Nkd1 impairs mouse spermatogenesis. J Biol Chem 2005; 280:2831–2839.
49. Jeays-Ward K, Dandonneau M, Swain A. Wnt4 is required for proper male as well as female sexual development. Dev Biol 2004; 276:431–440.
50. Ma P, Wang H, Guo R, Ma Q, Yu Z, Jiang Y, Ge Y, Ma J, Xue S, Han D. Stage-dependent Dishevelled-1 expression during mouse spermatogenesis suggests a role in regulating spermatid morphological changes. Mol Reprod Dev 2006; 73:774–783.
51. Kohn MJ, Kaneko KJ, DePamphilis ML. DkkL1 (Soggy), a Dickkopf family member, localizes to the acrosome during mammalian spermatogenesis. Mol Reprod Dev 2005; 71:516–522.
52. Weber JE, Russell LD, Wong V, Peterson RN. Three-dimensional reconstruction of a rat stage V Sertoli cell: II. Morphometry of Sertoli-Sertoli and Sertoli-germ cell relationships. Am J Anat 1983; 167:163–179.
53. Allan DJ, Harmon BV, Roberts SA. Spermatogonial apoptosis has three morphologically recognizable phases and shows no circadian rhythm during normal spermatogenesis in the rat. Cell Prolif 1992; 25:241–250.
54. Furuchi T, Masuko K, Nishimune Y, Obinata M, Matsui Y. Inhibition of testicular germ cell apoptosis and differentiation in mice misexpressing Bcl-2 in spermatogonia. Development 1996; 122:1703–1709.
55. Kubota H, Avarbock MR, Brinster RL. Growth factors essential for self-renewal and expansion of mouse spermatogonial stem cells. Proc Natl Acad Sci U S A 2004; 101:16489–16494.
56. Mishina Y, Rey R, Finegold MJ, Matzuk MM, Josso N, Cate RL, Behringer RR. Genetic analysis of the Mullerian-inhibiting substance signal transduction pathway in mammalian sexual differentiation. Genes Dev 1996; 10:2577–2587.
57. Behringer RR, Finegold MJ, Cate RL. Mullerian-inhibiting substance function during mammalian sexual development. Cell 1994; 79:415–425.
58. Behringer RR, Cate RL, Froelick GJ, Palmiter RD, Brinster RL. Abnormal sexual development in transgenic mice chronically expressing Mullerian-inhibiting substance. Nature 1990; 345:167–170.